In vivo local determination of tissue optical properties

F. Bevilacqua[a], D. Piguet[a], P. Marquet[a], J.D. Gross[b], B.J. Tromberg[b] and C. Depeursinge[a]

[a]Institut d'Optique Appliquée, Département de Microtechnique,
Ecole Polytechnique Fédérale de Lausanne, CP 127, 1015 Lausanne, Switzerland

[b]Beckman Laser Institute and Medical Clinic, University of California at Irvine
1002 Heath Sciences Road
Irvine CA 92612, USA

ABSTRACT

Local and superficial optical characterization of biological tissues can be achieved by measuring the spatially resolved diffuse reflectance at small source-detector separations. The sensitivity of the signal to the phase function, absorption and scattering coefficients were studied using Monte Carlo simulations. Measurements of spatially resolved reflectance were performed *in vivo* on human brain with source-detector separations from 0.3 to 1.5 mm. Distinct optical properties were found between normal cortex, astrocytoma of optic nerve and normal optic nerve.

Keywords: optical properties, absorption coefficient, scattering coefficient, turbid media, tissue optics, optical biopsy.

1. INTRODUCTION

Probing the optical properties of biological tissues has important consequences for medical diagnosis. Indeed, light scattering and absorption can provide information both on tissue structure and chromophore content, features which can be used to distinguish between normal tissues and malignant lesions. Several methods have already been proposed to quantitatively determine the absorption and reduced scattering coefficients *in vivo*, using spatially- and/or temporally-resolved measurements[1,2,3,4]. However these approaches employ probes with source-detector separations typically in the range of one centimeter or more, which implies that the depth of tissue probed is of the same order of magnitude. Our goal is to localize optical properties with high spatial precision using spatially resolved reflectance probes that have small source-detector separations (<2 mm). Such techniques have a great potential for optical biopsy[5].

The spatially resolved reflectance is denoted R(r) where r is the source-detector separation. The optical properties of tissues are defined by the absorption coefficient μ_a, the scattering coefficient μ_s, the phase function $p(\cos\theta)$ and the average index of refraction n of the medium. The phase function is the density probability function for the scattering angle θ. It can be expanded as follows[6]:

$$p(\cos\theta) = \frac{1}{4\pi}\sum_i (2i+1) m_i P_i(\cos\theta) \qquad (1)$$

where $P_i(\cos\theta)$ is the Legendre polynomial of order i and m_i is called the moment of order i. The first moment of $p(\cos\theta)$ is the mean cosine of θ, denoted g.
A commonly used phase function in tissue optics is the Henyey-Greenstein phase function defined by:

$$p(\cos\theta) = \frac{1}{4\pi}\frac{1-g^2}{(1+g^2-2g\cos\theta)^{1.5}} \qquad (2)$$

The moments of the Henyey-Greenstein phase function are $m_i=g^i$.
It is also useful to define the reduced scattering coefficient $\mu_s'=\mu_s(1-g)$ and the transport mean free path $mfp' = 1/(\mu_s'+\mu_a)$.

For further author information-
e-mail: frederic.bevilacqua@epfl.ch, tel.:+ 41 21 693 37 30, fax: + 41 21 693 37 01

SPIE Vol. 3194 • 0277-786X/98/$10.00

2. MATERIALS AND METHODS

2.1. Spatially-resolved measurement

The probe used for the measurement of the spatially resolved reflectance is described in Fig. 1. It is a linear array of optical fibers (core diameter of 200 µm, N.A.=0.37). Two fibers can be alternatively used to illuminate the tissue. The illuminating fibers are slid in small stainless steel tubes in order to avoid direct light coupling with the collecting fibers. The bundle is set in a stainless steel tube of 2.2 mm diameter and 20 cm long. The probe is rigid, which allows an easier handling by the physician. The whole probe can be sterilized.

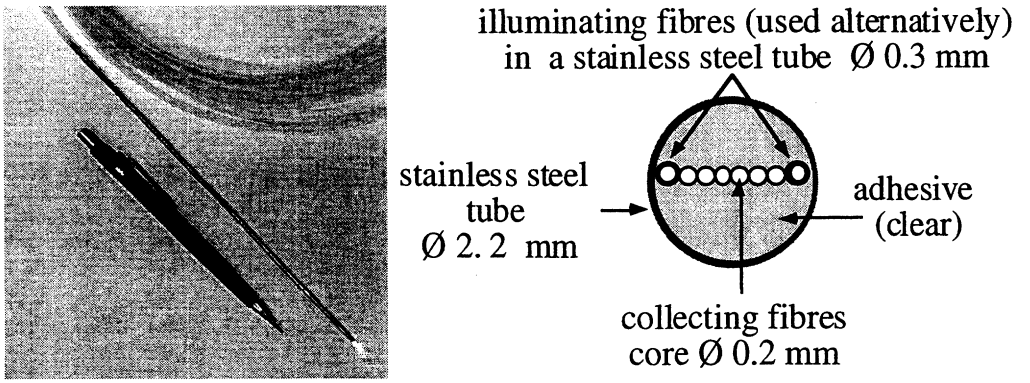

fig1. Probe for the measurement of the spatially resolved reflectance

The experimental set-up is shown in Fig.2. An optical switch allows to choose for each illuminating fiber three different sources: laser diodes emitting at 674 nm, 849 nm and 956 nm. The six fibers used to collect the backscattered light are imaged on a linear Charge-Coupled-Device (CCD). Only one measurement is then needed to get simultaneously the intensity of the six fibers. The set-up is driven by a PC computer.

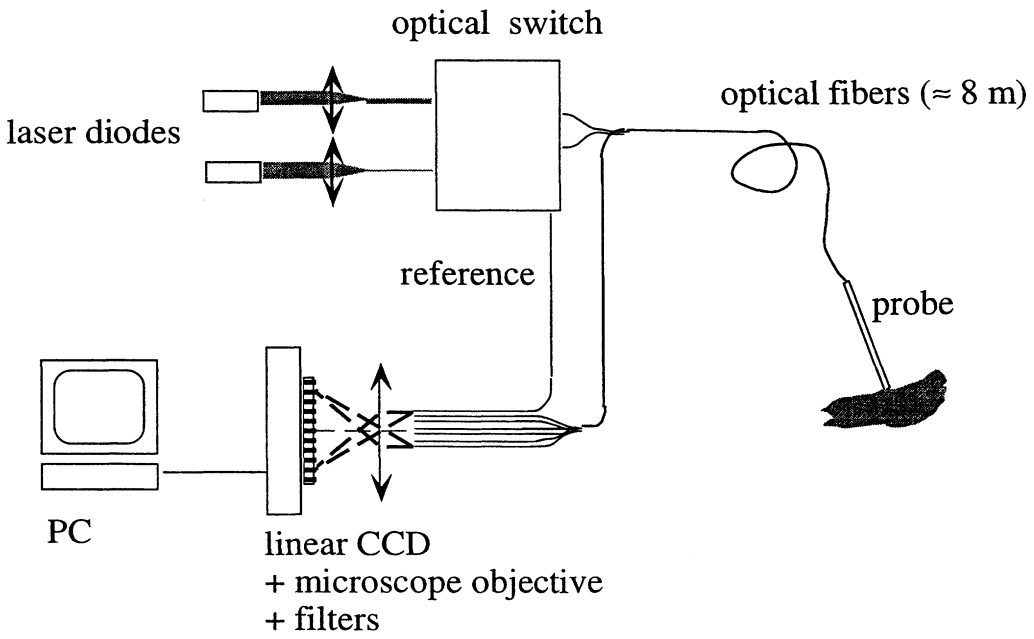

fig2. Experimental set-up

2.2. Calibration

First, the differences of transmission between each fiber are corrected using a measurement on a turbid phantom illuminated uniformly. Second, the absolute intensity is calibrated by a measurement on a solid turbid phantom in silicone of known optical properties. The calibration factor is defined by fitting the phantom measurement to the results of a simulation computed with the phantom coefficients. The coefficients μ_s' and μ_a of the phantom were measured by a frequency domain photon migration technique[3].

2.3. Monte Carlo Simulations

A model of photon migration in tissues is necessary to explicit the relationship between the measured reflectance and the optical properties. Analytical solutions from the diffusion equation are not appropriate in our case because we are interested in the reflectance close to the source, at distance comparable to the transport mean free path mfp'[1]. We performed Monte Carlo simulations to predict the measured reflectance of an homogeneous semi-infinite turbid media. The code we used was extensively tested in other configurations[7,8]. Our simulations take into account the exact diameter of the illuminating and collecting fibers, as well as their numerical apertures. The mismatch of index of refraction between the tissue (assumed to be n=1.4)[9] and the probe (n=1.5) is also taken into account.

3. RESULTS

3.1. Comparison between experiments and simulations

Experiments on microsphere suspension (polystyrene sphere Ø 1.072 ± 0.019 µm) were performed to assess the accuracy of our theoretical model. The scattering coefficient and the phase function of these suspensions were derived from Mie theory[10]. As no dye was added to the suspension, μ_a was considered to be equal to the water absorption. In Fig.3 two measurements of the reflectance are compared to a simulation computed with the microsphere suspension coefficients (μ_s'=1 mm^{-1}, μ_a=0.0005 mm^{-1}, g=0.92). The good agreement found here between experiments and simulation confirms the accuracy of our simulations. Note that no fitting parameter was used here, which proves the validity of our calibration procedure.

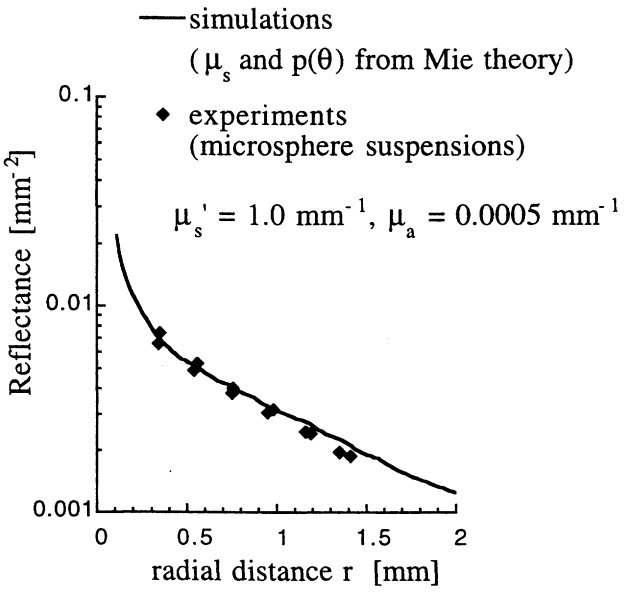

Fig.3. Comparison between experiments on microsphere suspension and Monte Carlo simulation.

3.2. Depth of tissue investigated

To quantify the volume of tissue probed by our technique, the average depth of scattering event was recorded for each detected photon. We present in Fig.4 the probability density function of this quantity for typical optical properties of tissues: μ_s'=1 mm^{-1}, μ_a=0.005 mm^{-1}, Henyey-Greenstein phase function with g=0.92. Fig.4 shows that tissues located below 2 mm are not playing a significant role in the measured signal by our probe (for r < 1.5 mm). This confirms that our measurements are mainly sensitive to the part of tissue located approximately within 1 mm below the surface. Thus the investigated volume is of the order of 1 mm^3.

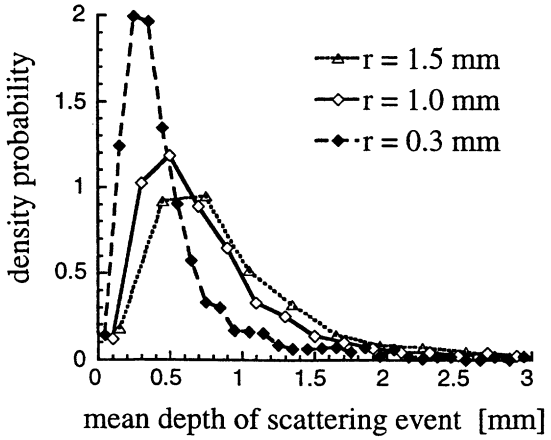

Fig.4 . Density probability function of the average depth of scattering event for three source-detector separations r. μ_s' = 1 mm^{-1}, μ_a = 0.005 mm^{-1} and g = 0.92.

3.3. Role of the phase function

It is well known that far from the source (r >> *mfp'*) the diffusion approximation is valid and only the first moment g of the phase function plays a role in the spatially-resolved reflectance[1,2]. In this case the spatially-reflectance depends only on two parameters: μ_a and $\mu_s'=\mu_s(1-g)$, which are usually used to characterize a given tissue. In contrast, close to the source (r ≈ *mfp'*) it is expected that higher order moments of the phase function have to be considered. To study this, the spatially resolved reflectance was computed for different phase functions (Fig.5 and Fig.6).

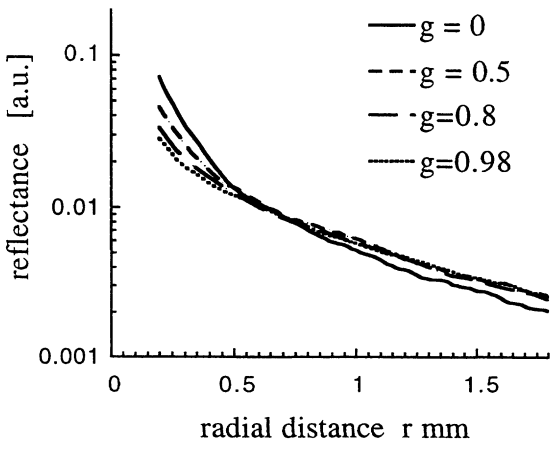

Fig.5. Reflectance simulated with different Henyey-Greenstein phase function. μ_s' = 1 mm^{-1}, μ_a = 0 mm^{-1}

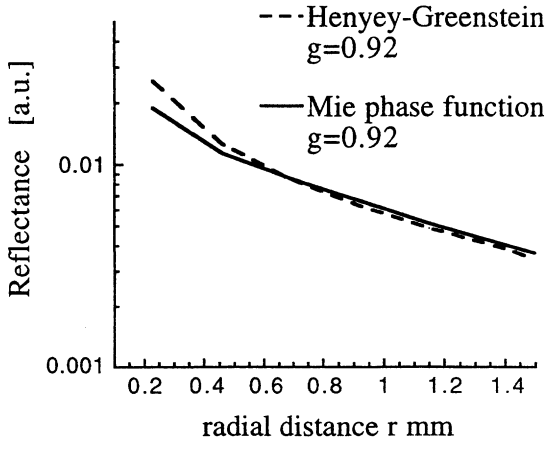

Fig.6. Reflectance simulated with two different phase functions with identical g=0.92.
μ_s' = 1 mm-1, μ_a = 0 mm^{-1}.

In Fig.5 the reflectance related to Henyey-Greenstein phase functions with values of g from 0 to 0.98 are reported. Significant differences are found in the reflectance between isotropic (g=0) and forward scattering with g>0.5 for r < 1.5 mfp'. However, difference smaller than 5% are found for distance larger than 0.5 mfp' for value of g between 0.5 and 0.98, which are typical values for tissues.
Nevertheless it should be noted that changing the parameter g in the Henyey-Greenstein phase function affects not only the first moment g but also all the other moments (the values of which are g^i where i the order of the moment). Thus, the discrepancy found in Fig.5 is not due only to differences in the first moment (anisotropy factor) but also to differences in moments of higher order. To demonstrated this, simulations with a Henyey-Greenstein phase function and a Mie phase function with identical first moment g=0.92 but different higher order moments are compared (Fig.6). Similarly to Fig.5 differences larger than 5% are found for distances smaller than 0.5 mfp' in Fig.6.

3.4. Role of μ_a and μ_s'

Two parameters are derived from the reflectance to quantify the effect of μ_s' and μ_a: the intensity of the reflectance at 1 mm from the source R(r=1 mm) and the slope of the logarithm (base e) of the reflectance at 1 mm from the source ∂_rlnR(r=1 mm). Here all the simulations results are related to the Henyey-Greenstein phase function with g=0.92, which is usually considered as a good approximation for biological tissues. Other phase functions sufficiently close to this one should not induce too important differences on the reflectance at 1 mm, and consequently on the two parameters R(r=1 mm) and ∂_rlnR(r=1mm) (see section 3.3.).

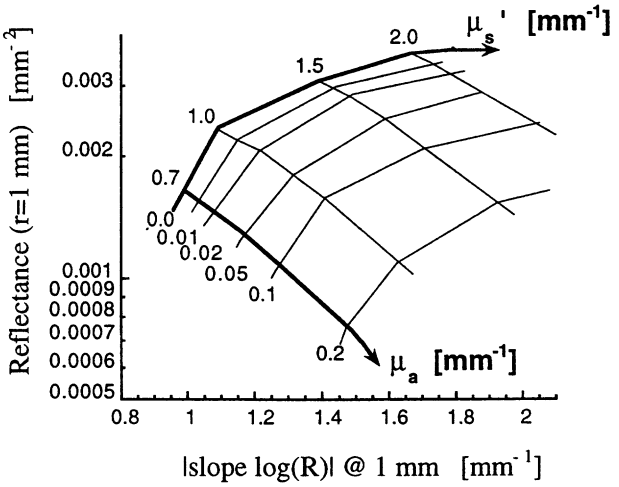

fig. 7. Relationship between the parameters (R(r=1), ∂rlnR(r=1mm)) and (μs', μa) for the Henyey-Greenstein phase function g=0.92.

Fig.7 shows graphically the relationship between (μ_s', μ_a) and the two parameters (R(r=1), ∂_rlnR(r=1mm)). Fig.7 clearly demonstrates that, for a given phase function, the two parameters (R(r=1), ∂_rlnR(r=1mm)) allow the determination of μ_a and μ_s'. As expected the sensitivity of μ_a is weak compared to methods using larger source detector separation. Uncertainties lower than 1% on R(r=1 mm) and ∂_rlnR(r=1mm) would be required to resolve μ_a<0.01 mm^{-1}. Such precision is difficult to achieve during *in vivo* measurements due to movements of the probe and heterogeneity of the tissues. Nevertheless μ_s' can be determined with a good precision. Uncertainties of 2% on R(r=1 mm) and ∂_rlnR(r=1mm) lead to uncertainties of approximately 5% on μ_s' and 20% on μ_a for μ_s' and μ_a close to 1 mm^{-1} and 0.05 mm^{-1} respectively.

3.5. *In vivo* measurements on brain tissues

Clinical measurements were recorded during brain surgery[11]. These data are analyzed assuming that the tissue phase function is close to the Henyey-Greenstein g=0.92. In Fig.8 the two parameters (R(r=1), ∂_rlnR(r=1mm)) obtained experimentally are superimposed on the grid already shown in Fig.7.
Several measurements were always performed successively at a given location. The fluctuations over these measurements were mainly due to probe movements. The average reflectance was calculated for each location, as well as the standard deviation. Note that the uncertainty due to the instruments, estimated from measurements on a phantom, are much lower (typically 2%).

Two set of measurements were performed on normal cortex, one on the temporal lobe and one on the frontal lobe. The values of μ_a and μ_s' obtained in these two cases are very close: μ_s' is 1 ± 0.1 mm^{-1} at 674 nm and decrease to 0.85 ± 0.1 mm^{-1} at 956 nm. The absorption is lower than 0.02 mm^{-1} for wavelength between 674 nm and 956 nm. Such lower absorption cannot be determined more precisely with our technique as it was discussed in section 4.4. Some points are even outside the grid which can be explained by two reasons: the actual phase function is strongly different from the one used in simulation, or the heterogeneity of the tissues perturbs the measured reflectance.
Two other sets of measurements were performed on a tumor (astrocytoma of optic nerve) and on the normal optical nerve. The normal optical nerve gives higher μ_s' (μ_s' $=1.8 \pm 0.1$ mm^{-1} at 674 nm) compared to the cortex and the tumor. The μ_s' of the tumor is similar to the cortex at λ=956 nm: μ_s' $=0.85 \pm 0.1$ mm^{-1}. However the variation of μ_s' between λ=674 nm and λ =956 nm is much larger for the tumor than for the cortex: $\mu_s'(\lambda = 956\ nm) - \mu_s'(\lambda = 674\ nm) \cong 0.55$ mm^{-1} for tumor, $\mu_s'(\lambda=956\ nm) - \mu_s'(\lambda=674\ nm) \cong 0.15$ mm^{-1} for the cortex. Such spectroscopic variation could be attributed to differences of the scatterer types. Another striking difference between the different type of tissues are related to absorption: the tumor exhibits a much higher absorption (of the order of 10) compared to cortex, certainly due to a higher hemoglobin content and vascularization.

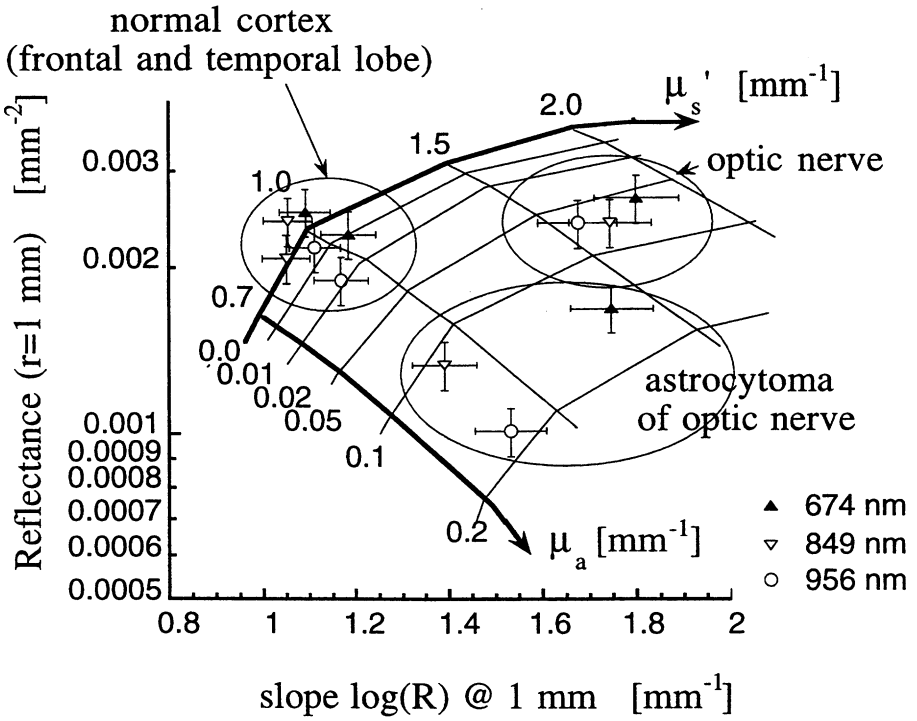

Fig.8 *In vivo* measurements on human brain

4. SUMMARY AND CONCLUSION

The purpose of this work was to assess the optical characterization of tissues by the measurement of the spatially resolved reflectance using short source-detector separation (< 2mm). Monte Carlo simulations, the accuracy of which was confirmed by experiments on microsphere suspensions, were used to establish the correspondance between the measured reflectance to the optical properties. Strong influence of the first and higher order moments of the phase function were demonstrated for distances smaller than one transport mean free path. Nevertheless, for a given phase function, μ_s' and μ_a can be determined by two parameters of the reflectance: R(r=1), $\partial_r \ln R(r=1mm)$. Simulations also showed that the depth probed by this technique is lower than 2 mm for typical biological tissues.

Finally *in vivo* measurements on human brain show that this technique allows an excellent discrimination between different types of tissues. The spectroscopic dependence of μ_s' as μ_a should lead to a better understanding of the scatterer properties and chromophore content of the different investigated tissues.

ACKNOWLEDGMENT

This work was supported by the Swiss National Science Foundation (N0 2053-049628.96), National Institutes of Health (NIH) Laser Microbeam and Medical Program (LAMMP) and Optical Biology facilities (grants, RR-01192 and CA-62203, respectively); NIH grant GM-50958, and DOE grant DE-FG03-91ER61227.

REFERENCES

1 . T. J. Farrell, M. S. Patterson and B. C. Wilson, "A diffusion theory model of spatially resolved, steady -state diffuse reflectance for the non invasive determination of tissue optical properties in vivo," Med.Phys. 19 879-888 (1992).

2 . R. Bays, G. Wagnières, D. Robert, D. Braichotte, J.-F. Savary, P. Monnier and H. van den Bergh, "Clinical determination of tissue optical properties by endoscopic spatially resolved reflectometry," Appl.Opt. 35 (10), 1756-1766 (1996).

3 . J.B. Fishkin, O. Coquoz, E.R. Anderson, M. Brenner and B. J. Tromberg, "Frequency-domain photon migration measurements of normal and malignant tissue optical propeties in human subject," Appl. Opt. 36 (1), 10-20 (1997).

4 . G. Mitic, J. Kölzer, J. Otto E. Plies, G. Sölkner and W. Zinth, "Time-gated transillumination of biological tissues and tissuelike phantoms," Appl.Opt. 33 (28), 6699-6710 (1994).

5 . J.R. Mourant, I.J. Bigio, J. Boyer R. L. Conn, T. Johnson and T. Shimada, "Spectroscopic Diagnosis of Bladder-Cancer with Elastic Light-Scattering," Lasers Surg. Med. 17 (4), 350-357 (1995).

6 . H.C. van de Hulst, *Multiple Light Scattering, Tables, Formulas, and Applications*, Academic Press. Inc., London, 1980.

7 . P. Marquet, F. Bevilacqua, C. Depeursinge and E. B. d. Haller, "Determination of reduced scattering and absorption coefficients by a single charge-coupled-device array measurement, part I: comparison between experiments and simulations," Opt.Eng. 34 (7), 2055-2063 (1995).

8 . F. Bevilacqua, P. Marquet, O. Coquoz and C. Depeursinge, "Role of tissue structure in photon migration through breast tissues," Appl.Opt, 36 (1), 44-51 (1997).

9 . F.P. Bolin, L.E. Preuss, R.C. Taylor and J. Ference, "Refractive index of some mammalian tissues using a fiber optic cladding method," Appl. Opt. 28 (12), 2297-2296 (1989).

10 . F. Bohren and D.R. Huffman, *Absorption and Scattering of Light by Small Particles*, Wiley, New York, 1983.

11 . Protocol and informed consent was obtained for the patient undergoing neurological surgery for an intra-axial brain tumor as demonstrated on conventional neuroimaging. The protocol and informed consent documents were approved by the UCI review board (HS#96-495).